INSTITUTE OF PHYSICS PUBLISHING JOURNAL OF PHYSICS: CONDENSED MATTER

J. Phys.: Condens. Matter **15** (2003) 2301–2307 PII: S0953-8984(03)58915-9

Trapping of oxygen vacancies on twin walls of $CaTiO_3$: a computer simulation study

Mark Calleja[1], **Martin T Dove and Ekhard K H Salje**

Mineral Physics Group, Department of Earth Sciences, University of Cambridge, Downing Street, Cambridge CB2 3EQ, UK

E-mail: mcal00@esc.cam.ac.uk

Received 29 January 2003
Published 31 March 2003
Online at stacks.iop.org/JPhysCM/15/2301

Abstract

We have studied the atomic structure of [001]90° rotation twin walls in orthorhombic $CaTiO_3$ (symmetry $Pbnm$) at low temperature (10 K) and their effects on oxygen vacancies. The wall thickness was found to be 2.3 nm at $T \ll T_c$ and it was found that it is energetically favourable for such vacancies to reside in the wall, particularly when bridging titania ions in the (001) plane. The binding energy of an oxygen vacancy in the wall with respect to the bulk is calculated to be $\leqslant 1.2$ eV.

1. Introduction

Twin walls in solids can play an important role in affecting transport properties within the host medium [1–3]. Examples are the enhanced transport of oxygen [4] and sodium [5] along twin walls in ferroelastic WO_3. Such walls can also inhibit ionic conductivity as we recently showed in the case of α-quartz [6], or may act as conduits for diffusion in a similar manner, seen at grain boundaries (see [7]). Since twin walls arise from well-defined displacive phase transitions, with widths that are controlled by temperature and orientations that are controlled by the crystal structure, they may provide a route to producing new materials with tailored chemical microstructure. However, a knowledge of the interaction between twin walls and inherent defects within the material, such as vacancies, then becomes important. For example, a recent experimental study using the technique of dynamical mechanical analysis on the perovskite $LaAlO_3$ concludes that domain walls in that system are pinned predominantly by oxygen vacancies [8]. The same authors also find evidence for domain walls in the perovskite $Ca_{1-x}Sr_xTiO_3$ being strongly pinned by vacancies at the O position [9]. Similarly, Wang *et al* [10] studied the internal friction in the ceramic Pb(Zr, Ti)O_3, finding oxygen vacancies responsible for the pinning of domain wall motion.

[1] www.esc.cam.ac.uk/minsci

Table 1. Potential parameters used in this work.

Interaction	A_{ij} (eV)	b_{ij} (Å^{-1})	C_{ij} (eV Å^6)	Charge q
O–O	22 764.0	6.7114	27.88	$q_{\mathrm{O}} = -2$
Ti–O	3 242.124	3.4626	0.0	$q_{\mathrm{Ti}} = 4$
Ca–O	2 272.741	3.3490	0.0	$q_{\mathrm{Ca}} = 2$

Recently, it has become a practical possibility to study domain walls using atomistic computational techniques. For example, ferroelectric domain walls in the perovskite $PbTiO_3$ have been studied using a first-principles ultrasoft-pseudopotentials approach, where it was found that 90° walls have energies a factor of four lower than their 180° counterparts [11]. Similarly, Mishin [12] has proposed a Monte Carlo method for calculating activation energies which we have implemented in a study of diffusion of alkali cations along domain walls in quartz [13].

In this paper, we investigate the energies associated with oxygen vacancies in the vicinity of twin walls in orthorhombic $CaTiO_3$. This phase is obtained experimentally by cooling through a displacive phase transition from the parent cubic perovskite phase [14, 15]. As a result of this transition, there are a number of different types of twin walls [16]. It is the aim of this work is to study the properties of oxygen vacancies in the neighbourhood of the [001]90° rotation twins. We were particularly interested to see whether the vacancies would preferentially reside on the wall or in the bulk.

2. Simulation details

2.1. Potentials

The simulation methods chosen here utilize empirical potentials. Although such techniques are not generally as accurate as modern *ab initio* methods, practical constraints due to system size favoured this strategy. The interatomic potentials used here are Buckingham and Coulombic potentials, to represent short-range and long-range interactions respectively. They have the following functional form for ions i and j separated by distance r:

$$V(r) = A_{ij}\exp(-b_{ij}r) - \frac{C_{ij}}{r^6} + \frac{q_i q_j}{4\pi\epsilon_0 r}. \tag{1}$$

We used the parameters given in table 1, with cut-off distances of 10 Å on the short-range interactions. The O–O potentials were taken from previous work on quartz [17]; this procedure has in fact been used for many studies of different oxides. The Ca–O potentials were taken from the modified electron gas calculations of Post and Burnham [18]. Initial parameters for the Ti–O interaction were also taken from this source, but the value of the A-parameter was adjusted to give the best agreement with the crystal structure using the program GULP [19]. The calculated values of the lattice parameters a, b and c are 5.388, 5.433 and 7.651 Å respectively, which compare well with experimental values of 5.380, 5.440 and 7.639 Å (maximum error 0.2%). As a further check, we measured the three rotation angles for the Ti octahedra between the experimental and fitted structures, finding all rotations to lie in the range $0.75° < \theta < 1°$.

As a test of these potentials we conducted a number of molecular dynamics runs using DL_POLY [20] in the $N\sigma T$ ensemble at various temperatures and 0 GPa. Figure 1 displays the scaled lattice constants $a/\sqrt{2}$, $b/\sqrt{2}$ and $c/2$ as the temperature is increased over the range 200–1600 K. Clearly the simulation shows a displacive phase transition to a cubic phase in the range 1300–1400 K. Experimentally, one observes the orthorhombic-to-tetragonal transition

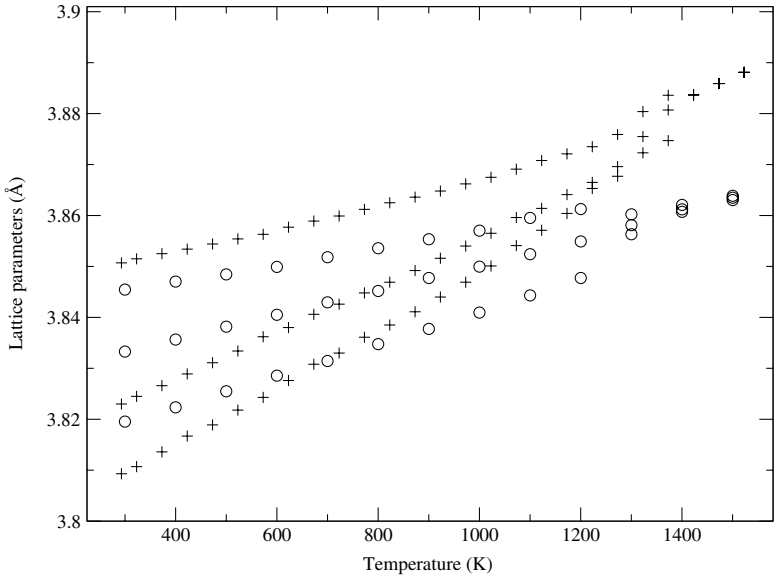

Figure 1. The T-dependence of the lattice constants. Circles are from our model potentials and crosses are experimental data from [14]. In each case, the top set corresponds to $b/\sqrt{2}$, the middle set to $c/2$ and the bottom set to $a/\sqrt{2}$.

$Pbnm \leftrightarrow I4/mcm$ at $T_c = 1373$–1423 K and ambient pressure, before reaching the cubic $Pm\overline{3}m$ state at ∼1523 K [14]. We may be missing the narrow tetragonal phase due to the simplicity of the potentials used. The general agreement is quite good, although the ratios of the lengths are not quite correct.

2.2. Monte Carlo details

We now describe the methodology employed for investigating twinned structures. For this work we developed our own Monte Carlo code [13], based on the Metropolis sampling scheme [21]. The system comprised 7800 ions with orthorhombic periodic boundary conditions. An initial, defect-free, configuration was equilibrated in the isothermal–isobaric (NPT) ensemble at 10 K and 0 GPa. The required vacancies were then introduced and the subsequent simulations were performed in the canonical (NVT) ensemble. Charge balancing was achieved by removing a calcium ion far from the oxygen vacancy, which was made possible by the size of the models studied. Alternative schemes for smaller configurations based on jellium models exist [7] but were not necessary here. Each vacancy simulation was further equilibrated for ∼1000 cycles before the statistics were gathered. We define a cycle here as one attempted move for every ion in the configuration.

3. Domain wall formation

The structure of a [001]90° rotation twin wall was simulated by suitably aligning two bulk regions which had been rotated relative to each other, and then equilibrating the system. A view of the relaxed model along [001] is shown in figure 2. The points are Ca^{2+} ions, while Ti^{4+} ions reside at the vertices of the solid lines and are bridged by O^{2-} ions. Note the two domain walls, one at the centre of the figure and the other at the extreme left-hand side. These can be

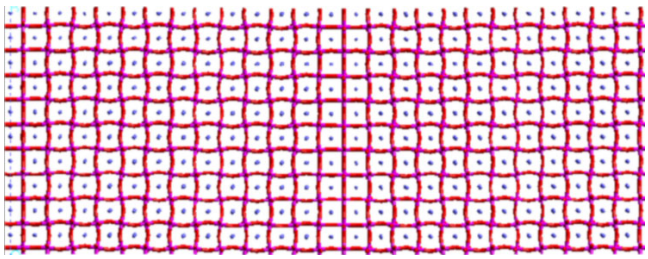

Figure 2. A view along the *c*-axis of an equilibrated configuration. Titania ions reside at the vertices of the solid lines, and are bridged by oxygen ions. The points are calcium ions. Note the walls at the centre and extreme left of the diagram.

(This figure is in colour only in the electronic version)

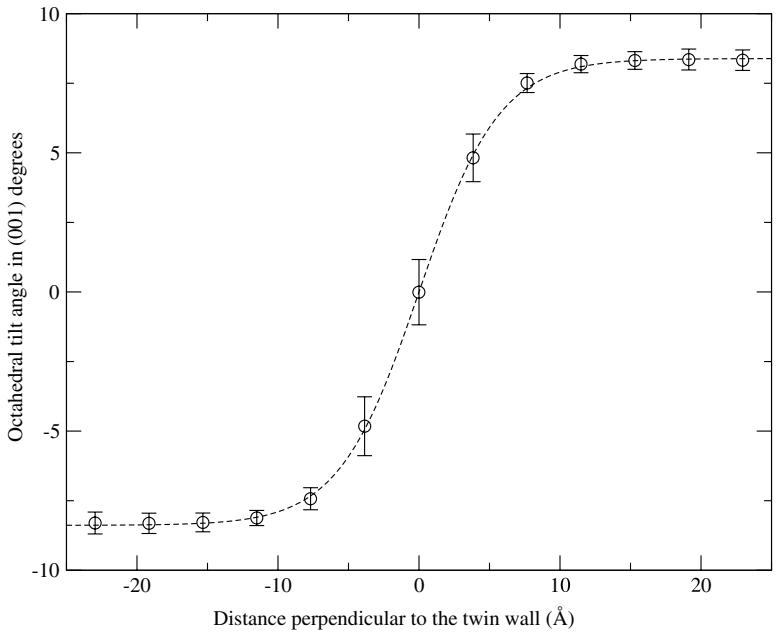

Figure 3. The order parameter profile for orthorhombic $CaTiO_3$. The points are simulation data at 10 K, while the curve is a fit to $y = \alpha \tanh(\gamma x)$ (see the text).

discerned as straight lines running from the bottom to the top of the figure, and correspond to a zero rotation of the Ti^{4+} octahedra in the (001) plane.

The empirical potentials used in this study result in a wall energy of 0.32 ± 0.02 J m^{-2} in the $T \rightarrow 0$ K limit. This value was calculated by comparing the potential energies of the twinned and untwinned crystals. It is comparable to the values calculated for other perovskite structures using Landau–Ginzburg theory [22]. The wall thickness can be deduced by calculating an order parameter profile for the sample. Such a quantity is zero in the high-symmetry phase in the wall and non-zero in the lower-symmetry bulk. The attribute chosen here is the tilt angle made by the titania octahedra in the (001) plane. A plot of this quantity is shown in figure 3 and leads to a wall thickness of 2.3 nm as $T \rightarrow 0$ K. For such a twinned system with order parameter Q,

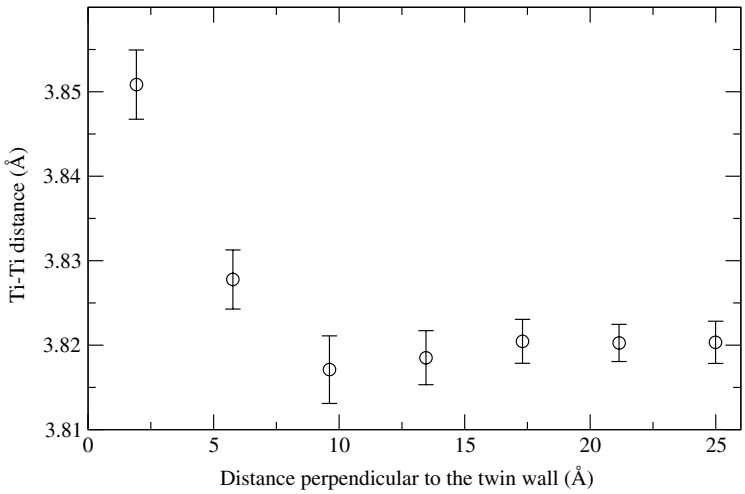

Figure 4. Ti–Ti nearest-neighbour distances perpendicular to a wall. The wall is at the origin.

the Landau potential has the form [22]

$$L(Q) = AQ^2(x) + BQ^4(x) + g\left(\frac{\mathrm{d}Q}{\mathrm{d}x}\right)^2 \qquad A < 0;\ B, g > 0. \tag{2}$$

This leads to the profile

$$Q(x) = \sqrt{\frac{-A}{2B}}\tanh\left(\sqrt{\frac{-A}{2g}}x\right). \tag{3}$$

Such behaviour can be seen from the fit to our simulation data with the function $Q = \alpha\tanh(\gamma x)$, obtaining $\alpha = 8.387$ and $\gamma = 0.176$ Å^{-1}, which gives a wall width at half-height of $w = 2/\gamma = 11.364$ Å.

Figure 4 shows the average Ti–Ti distances for nearest neighbours relative to a wall. Note how these distances are forced to increase by ∼0.7% at the wall due to the straightening of the Ti–O–Ti bonds. This increase would help reduce the steric hindrance experienced by an ion diffusing along the wall, implying greater ionic conductivity within the plane of the wall, e.g. via a vacancy-hopping mechanism. A detailed investigation of these processes will be reported elsewhere.

4. Vacancy calculations

We now consider the relative preference of oxygen vacancies in the vicinity of a twin wall, which is the main result of this paper. Figure 5 shows the change in crystal energy for single oxygen vacancies situated at various distances from the twin wall, starting in the wall and moving perpendicularly away from it towards the bulk region. The wall lies at the right-hand side of the figure. We plot the differences in crystal energy relative to the lowest-energy point within the wall. There are in fact three sets of data plotted, one for each possible direction of a bridging oxygen. Within the wall these directions are simply the cartesian directions, but become tilted away as we move into the bulk due to the rotations of the Ti octahedra.

It is evident that it is more energetically favourable for the vacancies to reside within the wall than in the bulk. The calculated energy difference is just under 1.25 eV, although this

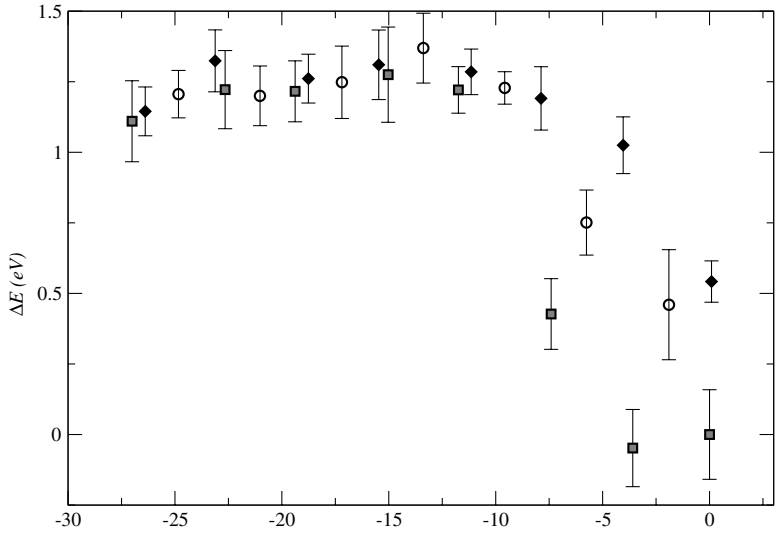

Figure 5. Relative crystal energy due to single oxygen vacancies. There is a twin wall at the origin. Circles denote vacancies for oxygens bridging titania along [100], squares those bridging along [010] and diamonds those bridging along [001]. The wall lies in (100).

may be a slight overestimation as our potential model cannot take into account any electronic relaxation that may occur due to the anisotropy introduced by a vacancy, as discussed in a recent study of oxygen vacancies in another perovskite, $BaTiO_3$, using embedded-cluster calculations [23]. In that work the small region around the vacancy is treated quantum mechanically, with the embedding lattice described by a pair potential model. The result is that isolated oxygen vacancies induce electronic deep-gap levels.

Figure 5 also indicates that in the vicinity of the wall, vacancies for oxygen ions bridging along the *c*-axis are considerably less likely than those in the (001) plane. This distinction disappears in the bulk. The inference here is that just as for the WO_3 twins mentioned in the introduction, [001]90° walls in orthorhombic perovskite are liable to display greater ionic conductivity than the bulk, the mechanism here being of the oxygen vacancy type. The relative preference for vacancies to reside within the wall could also provide a mechanism for the pinning of a wall.

Acknowledgments

We thank the EPSRC for funding this work, and S A T Redfern and R J Harrison for useful discussions.

References

[1] Salje E K H 1990 *Phase Transitions in Ferroelastic and Co-Elastic Crystals* (Cambridge: Cambridge University Press)
[2] Lee W, Salje E K H and Bismayer U 2003 *Phase Transit.* **76** 81
[3] Lee W, Salje E K H and Bismayer U 2003 *J. Phys.: Condens. Matter* **15** 1
[4] Aird A and Salje E K H 1998 *J. Phys.: Condens. Matter* **10** L337
[5] Aird A and Salje E K H 2000 *Eur. Phys. J.* B **15** 205
[6] Calleja M, Dove M T and Salje E K H 2001 *J. Phys.: Condens. Matter* **13** 9445

[7] Astala R and Bristowe P D 2002 *J. Phys.: Condens. Matter* **14** 6455
[8] Harrison R J and Redfern S A T 2002 *Phys. Earth Planet. Inter.* **134** 253
[9] Harrison R J, Redfern S A T and Street J 2003 *Am. Mineral.* **88** 574
[10] Wang C, Fang Q F, Shi Y and Zhu Z G 2001 *Mater. Res. Bull.* **36** 2657
[11] Meyer B and Vanderbilt D 2002 *Phys. Rev.* B **65** 104111
[12] Mishin Y 1997 *Defect Diffusion Forum* **143–147** 1357
[13] Calleja M, Dove M T and Salje E K H 2003 *Modell. Simul. Mater. Sci. Eng.* submitted
[14] Redfern S A T 1996 *J. Phys.: Condens. Matter* **8** 8267
[15] Kennedy B J, Howard C J and Chakoumakos B C 1999 *J. Phys.: Condens. Matter* **11** 1479
[16] Wang Y B and Liebermann R C 1993 *Phys. Chem. Minerals* **20** 147
[17] Sanders M J, Leslie M and Catlow C R A 1984 *J. Chem. Soc. Chem. Commun.* 1271
[18] Post J E and Burnham C W 1986 *Am. Mineral.* **71** 142
[19] Gale J D 1997 *J. Chem. Soc. Faraday Trans.* **93** 629
[20] Smith W, Yong C W and Rodger P M 2002 *Mol. Simul.* **28** 385
[21] Thijssen J M 1999 *Computational Physics* (Cambridge: Cambridge University Press)
[22] Salje E K H 2000 *Rev. Miner. Geochem.* **39** 65
[23] Donnerberg H and Birkholz A 2000 *J. Phys.: Condens. Matter* **12** 8239